



Application of WRF-Chem to simulate air quality over Northern Vietnam

Thi Nhu Ngoc Do¹ · Xuan Truong Ngo¹ · Van Ha Pham¹ · Nhu Luan Vuong² · Hoang Anh Le² · Chau Thuy Pham³ · Quang Hung Bui¹ · Thi Nhat Thanh Nguyen¹

Received: 10 October 2019 / Accepted: 16 April 2020 / Published online: 23 May 2020
© Springer-Verlag GmbH Germany, part of Springer Nature 2020

Abstract

The WRF-Chem (Weather Research and Forecasting with Chemistry) model is implemented and validated against ground-based observations for meteorological and atmospheric variables for the first time in Northern Vietnam. The WRF-Chem model was based on HTAPv2 emission inventory with MOZCART chemical-aerosol mechanism to simulate atmospheric variables for winter (January) and summer (July) of 2014. The model satisfactorily reproduces meteorological fields, such as temperature 2 m above the ground and relative humidity 2 m above the ground at 45 NCHMF meteorological stations in January, but lower agreement was found in those simulations of July. PM₁₀ and PM_{2.5} concentrations in January showed good temporal and spatial agreements to observations recorded at three CEM air monitoring stations in Phutho, Quangninh, and Hanoi, with correlation coefficients of 0.36 and 0.59. However, WRF-Chem model was underestimated with MFBs from –27.9 to –118.7% for PM₁₀ levels and from –34.2 to –115.1% for PM_{2.5} levels. It has difficulty in capturing day-by-day variation of PM₁₀ and PM_{2.5} concentrations at each station in July, but MFBs were in the range from –27.1 to –40.2% which is slightly lower than those in January. It suggested that further improvements of the model and local emission data are needed to reduce uncertainties in modeling the distribution of atmospheric pollutants. Assessment of biomass burning emission on air quality in summer was analyzed to highlight the application aspect of the WRF-Chem model. The study may serve as a reference for future air quality modeling using WRF-Chem in Vietnam.

Keywords WRF-Chem · Air quality modeling · Northern Vietnam

Introduction

Particulate matter (PM) has become one of the most significant air pollutant concerns in developing Asian countries,

Responsible editor: Gerhard Lammel

Electronic supplementary material The online version of this article (<https://doi.org/10.1007/s11356-020-08913-y>) contains supplementary material, which is available to authorized users.

✉ Thi Nhu Ngoc Do
ngocdm@fimo.edu.vn

¹ University of Engineering and Technology, Vietnam National University Hanoi, 144 Xuan Thuy Road, Cau Giay, Hanoi, Vietnam

² Center of Environmental Monitoring, Vietnam Environment Administration, No. 10 Ton That Thuyet Street, Nam Tu Liem, Hanoi, Vietnam

³ Faculty of Environment, Vietnam National University of Agriculture, Trauquy, Gialam, Hanoi, Vietnam

including Vietnam, as it has negative impacts on human health (Stölzel et al. 2007; Anderson et al. 2012) and plays an important role on the atmosphere and climate system (IPCC 2013). Rapid population growth, industrialization, and urbanization result in high emissions of primary PM and major precursors for formation of secondary PM, ozone, and acid deposition in urban areas. In order to develop effective air quality management strategies, the current status of air quality should be understood and the relationship between source emission/meteorology and the atmospheric concentrations also should be analyzed.

In recent years, some large cities in Vietnam face high levels of air pollution, especially particulate matter concentrations. The national state of environmental report of 2016 showed that PM₁₀ and PM_{2.5} levels in urban areas are generally high and exceed national standards many days in each year between 2012 and 2016 (MONRE 2016). The current status and its mitigation in Vietnam were summarized in Nguyen et al. (2019b). In Vietnam, air pollution monitoring

has been mainly conducted by the Center for Environmental Monitoring (CEM), Vietnam Environment Administration (VEA), and Ministry of Natural Resources and Environment (MONRE). There are seven automatic continuous monitoring systems which were installed at road sites in six large cities/provinces, such as Hanoi, Quangninh, and Phutho (northern area) and Hue, Danang, and Nhatrang (middle area). Moreover, local government or other agencies (US and Germany Embassies in Hanoi and Hochiminh) have been recently investing their own environmental monitoring networks. Besides standard measurement instruments, low-cost sensors were considered as a potential good approach for Vietnam. As a result, a low-cost sensor network supported by Hanoi Environment Protection Agency and GIZ has been recently utilized to extend air pollution monitoring network in Hanoi (Nguyen et al. 2019a). However, ground observation data is still limited and represents site-specific characteristics; a large-scale and high-resolution monitoring of air quality in Vietnam is a challenge at the present.

Although the simplest technique for evaluating the spatial-temporal distribution of urban air pollution focused on interpolation of ambient concentrations from existing monitoring networks (Ferretti et al. 2008; Pérez Ballesta et al. 2008), there is a limited number of automatic continuous ground-level PM observations in Vietnam. Therefore, air quality models would provide a simplified view of air pollution at a large scale for air quality management, long-range transport, and health assessment study. Historically, there are two approaches, namely empirical/statistical and deterministic approach for air quality modeling (Collett and Oduyemi 1997). Based on the first, maps of PM_{2.5} concentrations over Hanoi between August 2010 and July 2012 (Nguyen et al. 2014) and Vietnam from December 2010 to September 2014 (Nguyen et al. 2015) have been estimated by using satellite images and ground-based measurements. However, the empirical/statistical approach is required long-time historical data and also unable to address the physical and chemical process of pollutants.

In contrast, the deterministic air quality models, which combine emission with meteorological and chemical atmospheric processes, have been led to more explainable forecasts. Three-dimensional chemical transport model (CTM) is one of deterministic air quality models that required more computation than empirical/statistical approach. Recently, CTMs developed to simulate air quality and applied in different parts of the world such as EMEP (Simpson et al. 2003), CAMx (Nopmongcol et al. 2012; Danh et al. 2016), CMAQ (Zhang et al. 2006, 2014; de Almeida Albuquerque et al. 2018), and CHIMERE (Bessagnet et al. 2008; Permadi et al. 2017). Those models have offline configuration in which meteorological and chemical processes are treated independently. This offline separation has not been able to simulate the feedbacks between air quality and climate/meteorology and may result in an incompatible and inconsistent coupling between

both meteorological and air quality models (Zhang 2008) and a loss of important information of atmospheric processes (e.g., wind speed and direction, cloud formation, and precipitation) (Grell et al. 2005). On the other hand, the online configuration in which meteorological and chemical processes are treated together on the same grid and with the same physical parameterizations thus feedbacks that mechanism can be considered (Grell and Baklanov 2011).

The online-coupled model systems have been applied extensively by science communities. Furthermore, the development of coupled meteorology-chemistry models was driven by the need for forecasting air quality in real-time, simulating feedbacks between air quality and regional climate, and responses of air quality to changes in future regional climate, land use, and biogenic emissions (Zhang 2008). The Weather Research and Forecasting Model with Chemistry (WRF-Chem) (Grell et al. 2005) represents the state-of-the-science global and regional online coupled model system applying increasingly over North America, Europe, and Asia in recent years (Kumar et al. 2012; Tuccella et al. 2012; Tessum et al. 2015; Mar et al. 2016; Zhong et al. 2016; Yahya et al. 2017; Georgiou et al. 2018).

In Vietnam, offline air pollution models are more widely used than online ones. CMAQ coupled with MM5 (The Penn State University (PSU)/NCAR mesoscale model) application is used for the next-day ozone forecasting in continental Southeast Asia including Hochiminh city on January 1–30, 2006 (Nghiem 2008). Another simulation was done by the CAMx/MM5 model system for a historical ozone episode in Hochiminh city in the period of March 1–13, 2005, and its evaluation with monitoring data. The modeling satisfied the US EPA-suggested criteria ranges during the period excluding the 3 days of low MM5 performance based on statistics averaged from three ground stations (Oanh 2013). A similar case study using CAMx/MM5 model for ozone simulation was conducted in Southern Vietnam (Danh et al. 2016). However, that study focused on assessment of rice yield loss due to ozone pollution without model skills evaluation. At a smaller scale, the UAM-V/SAIMM (variable-grid Urban Airshed Model combined with Systems Applications International (SAI) Mesoscale Model) system was utilized to simulate the formation and accumulation of surface ozone in the Hanoi metropolitan region domain during an ozone episode on March 3–4, 2003 (An 2005). Modeling PM₁₀ in Hochiminh city in 2012 was conducted by using a meteorology model named finite volume model (FVM) and transport and photochemistry mesoscale model (TAPOM) (Ho 2017).

On the other hand, the studies with online air quality models in Vietnam are very limited. Only one study applied WRF-Chem to simulate aerosol over Vietnam (Van et al. 2014). They successfully implemented the model with sensitivity studies of the chemical configuration and some qualitative assessment was presented. However, the statistical

analysis had not yet been done to evaluate the performance of air quality modeling for Vietnam due to the lack of monitoring data at that time.

In this paper, we report on the simulation of PM_{10} and $PM_{2.5}$ mass concentration in Northern Vietnam during 2014 winter and summer seasons, by the implementation of WRF-Chem. These modeled data were used for initial systematic validation against ground-based monitoring data. This work is thus aimed at a preliminary validation of the model for future operational applications. Furthermore, the impacts of biomass burning emission on air quality in summer were analyzed to emphasize an application aspect.

Data and methods

WRF-Chem configuration

WRF-Chem, which is the first public model developed by the National Oceanic and Atmospheric Administration (NOAA), Earth System Research Laboratory (ESRL), has been contributing by global science community. The Weather Research and Forecasting (WRF) is a mesoscale non-hydrostatic meteorological model. In the WRF-Chem model system, a version of the WRF model was coupled online with a chemistry model where meteorological and chemical components are predicted simultaneously. A detailed description of the model system is presented by Grell et al. (2005) and Fast et al. (2006).

In this work, we run the WRF-Chem model version 3.8.1 resealed in 2017 on three nested 36-, 12-, and 4-km resolution grids corresponding to 61×94 , 112×160 , and 154×148 cells, and 31 vertical layers. The innermost modeling domain (see Fig. 1) covers Northern Vietnam. The Lambert projection has been used according to the project specifications. We have conducted two simulations in January and July 2014, which represented for winter and summer time in North Vietnam, based on available ground observation data. This experiment was for evaluation of modeled meteorological and atmospheric PM_{10} and $PM_{2.5}$ concentrations with seasonal variation. In addition, further experiments that were built from May to middle of June including EXP_NOFINN (experiment without FINN) and EXP_FINN (experiment with FINN) to investigate the effects of biomass burning on air pollution. The hourly outputs were stored for analysis and the first 3 days of each simulation were discarded as model spin up.

This study utilizes chemical mechanisms MOZART-4 (Emmons et al. 2010). MOZART chemistry includes 81 chemical species participating in 159 gas phases and 38 photolysis reactions. Aerosols are represented using Global Ozone Chemistry Aerosol Radiation and Transport (GOCART) (Mian et al. 2000) with MOZART. The

photolysis rates are calculated using the Madronich Fast Tropospheric Ultraviolet-Visible (FTUV) scheme. Other settings and parameters employed for WRF-Chem in this study were detailed in Table 1. The physics options (i.e., microphysics, longwave radiation, shortwave radiation, surface layers, land surface, planetary boundary layer, cumulus parameterization) for the meteorology simulation (i.e., WRF) have been chosen in such a way that they are compatible with the chemistry and aerosol scheme in the WRF-Chem simulations (Mues et al. 2018).

In this study, output datasets based on MOZART-4 global simulations (Emmons et al. 2010) were used as chemical boundary conditions. These datasets are usually used as chemical boundary conditions in WRF-Chem (González et al. 2018; Mues et al. 2018). Currently, the information covers the period between January 1, 2007, and January 21, 2018, with a $1.9^\circ \times 2.5^\circ$ grid resolution and 56 vertical levels every 6 h. The MOZART-4 global model output for the year 2014 over the considered region was downloaded from <http://www.aocom.ucar.edu/wrf-chem/mozart.shtml>.

Topography, land use, and land water datasets were interpolated from USGS with the spatial resolution of each domain (5', 2', and 30" for d01, d02, and d03, respectively). Meteorological initial and boundary conditions are provided by the 6-h National Centers for Environmental Prediction (NCEP) FNL (Final) Operational Global Analysis data at a horizontal grid resolution of $1^\circ \times 1^\circ$ (<https://rda.ucar.edu/datasets/ds083.2/>).

Hemispheric Transport of Air Pollution (HTAP v2.2) emission inventory for the year 2010 (http://edgar.jrc.ec.europa.eu/htap_v2/index.php) was used as anthropogenic emission data. The emission data combines the latest available regional information within a complete global dataset. HTAP uses nationally reported emissions combined with regional inventories. The emission data are complemented with EDGAR v4.3 data for those regions with missing data. The global dataset is a joint contribution of the US Environmental Protection Agency (US-EPA), the MICS-Asia group, EMEP/TNO, the Regional Emission inventory in Asia (REAS), and the EDGAR group for scientific studies of hemispheric transport of air pollution. The HTAP dataset, providing emissions of CH_4 , CO, SO_2 , NO_x , non-methane volatile organic compounds (NMVOCs), NH_3 , PM_{10} , $PM_{2.5}$, black carbon (BC), and organic carbon (OC), is harmonized at a spatial resolution of $0.1^\circ \times 0.1^\circ$ and available with monthly time resolution. Further information was described in detail in Janssens-Maenhout et al. (2015). In the region in this study, the emissions are based on data from REAS (Kurokawa et al. 2013) which have a resolution of $0.25^\circ \times 0.25^\circ$. Biogenic emissions of trace species are calculated online using the Model of Emissions of Gases and Aerosols from Nature (MEGAN) (Guenther et al. 2012). Daily varying emissions of trace species from biomass

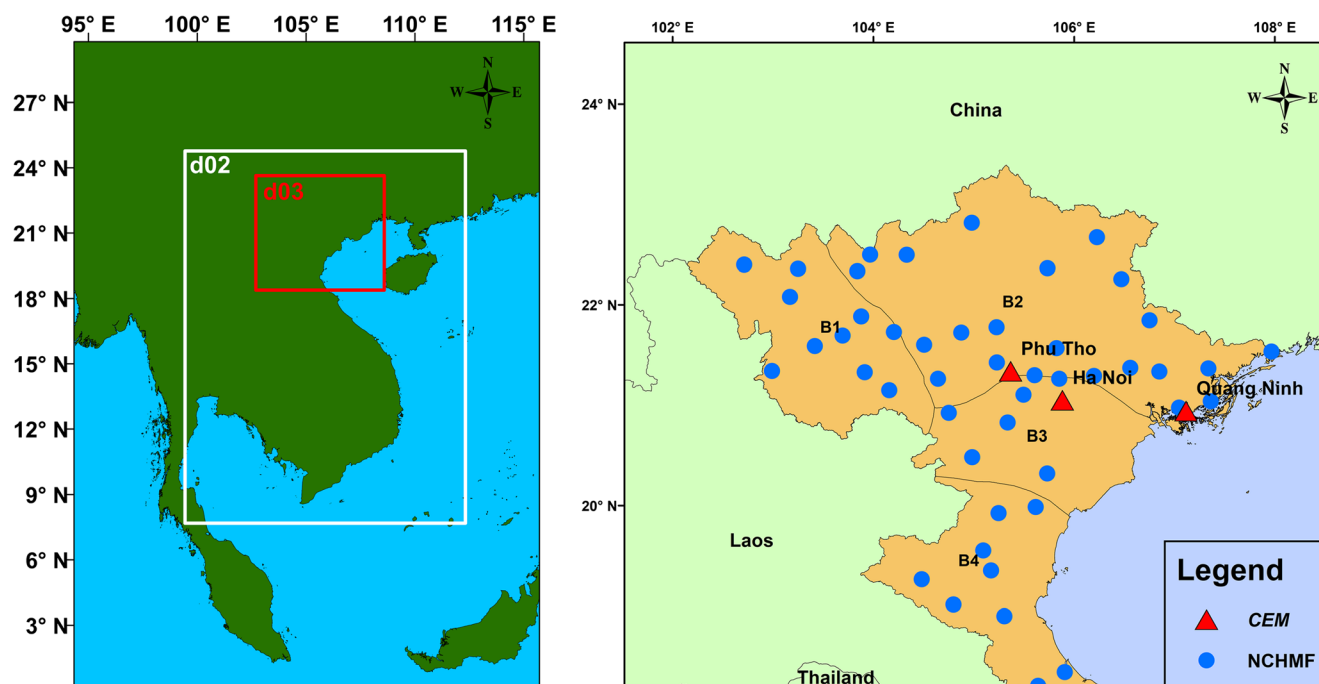


Fig. 1 WRF-Chem model domain (left) and ground-based stations over the domain d03 (right)

burning are provided to the model through the Fire Inventory from NCAR (FINNv1.5) (Wiedinmyer et al. 2011). Although these emission inventories have some uncertainty (Kurokawa et al. 2013; Janssens-Maenhout et al. 2015), it is generally difficult to evaluate such an emission inventory in Vietnam, due to the lack of completely bottom-up emission inventory. Their validation of these against actual emissions is beyond the scope of this work.

Table 1 Selected WRF-Chem settings and parameters employed in this study

| Category | Scheme |
|------------------------------|----------------------------|
| Physics options | |
| Microphysics | New Thompson et al. scheme |
| Longwave radiation | RRTMG scheme |
| Shortwave radiation | CAM scheme |
| Surface layers | MM5 similarity |
| Land surface | Noah Land Surface Model |
| Planetary boundary layer | Yonsei University PBL |
| Cumulus parameterization | Grell 3D |
| Chemistry options | |
| Gas-phase chemical mechanism | MOZART |
| Aerosol scheme | GOCART |
| Photolysis scheme | Madronich F-TUV |

Ground-based meteorological and PM data

In this study, the meteorological data from 45 stations of Vietnam National Centre for Hydro-Meteorological Forecasting (NCHMF) and three stations of Center for Environmental Monitoring (CEM) continuous observation stations were included to evaluate the model simulation for surface air temperature at 2 m above the ground (T2) and surface relative humidity at 2 m above the ground (RH2) in January and July of 2014. The near-surface concentration of PM₁₀ and PM_{2.5} mass from three CEM continuous observation stations were collected for validating the model outputs. All CEM stations are urban roadside stations. Figure 1 (right) shows the 45 NCHMF stations with blue dot and three CEM stations with red triangles, distributed into four climate sub-regions (i.e., Northwest region—B1, Northeast region—B2, Red River Delta region—B3, North Central region—B4) (Phan et al. 2009).

Active fire data

Fire datasets from May to June 2014 over Vietnam were obtained from the Visible Infrared Imaging Radiometer Suite (VIIRS) onboard Suomi NPP satellites. The datasets in a shapefile format were downloaded from the following link <https://firms.modaps.eosdis.nasa.gov/download/create.php>.

The VIIRS fire product is at a 375-m (I-bands) resolution every 12 h or less depending on the latitude. The VIIRS fire product provides the latitude and longitude of the fire pixels, the date and time of the fire detection, and fire radiative power (FRP) including confidence levels of fire detection. Specific to this study, we used all fires from each dataset to count without applying any confidence threshold.

Modeling evaluation

After matching all hourly observed values with their corresponding modeled values, we calculate metrics shown in Eqs. (1)–(6):

$$MB = \frac{1}{N} \sum_{i=1}^N (M_i - O_i) \tag{1}$$

$$MAGE = \frac{1}{N} \sum_{i=1}^N |M_i - O_i| \tag{2}$$

$$RMSE = \sqrt{\frac{1}{N} \sum_{i=1}^N (M_i - O_i)^2} \tag{3}$$

$$IOA = 1 - \left[\frac{N \times RMSE^2}{\sum_{i=1}^N (|M_i - O_i| + |O_i - O_i|)} \right] \tag{4}$$

$$MFB = \frac{2}{N} \sum_{i=1}^N \left[\frac{(M_i - O_i)}{(M_i + O_i)} \right] \times 100\% \tag{5}$$

$$MFE = \frac{2}{N} \sum_{i=1}^N \left[\frac{|M_i - O_i|}{(M_i + O_i)} \right] \times 100\% \tag{6}$$

where *i* corresponds to one of *n* measurement locations, *M* and *O* are the modeled and observed values, respectively, MB is the mean bias, MAGE is the mean absolute gross error, RMSE is the root-mean-square error, IOA is the index of agreement, MFB is the mean fractional bias, and MFE is mean fractional error. The slope (*S*), intercept (*I*), Pearson correlation coefficient (*r*), and squared Pearson correlation coefficient (*R*²) of a linear regression between modeled and measured values were additionally calculated.

For meteorological parameters, according to a report for the meteorological model MM5 over the continental US prepared for the US EPA (Emery et al. 2001), bias should be ≤ ± 0.5 K for temperature with a MAGE < 2 K and an IOA > 0.7, and bias should be ≤ 5% with a MAGE ≤ 10% (at 25 °C, 1 atm) and IOA > 0.7 for relative humidity. Besides, model performance goals and criteria have been published for PM (Boylan and Russell 2006). Goals reflect performance that models should strive to achieve while criteria reflect performance that

models should achieve to be used for regulatory purposes. The goals and criteria suggested by Boylan and Russell (2006) vary with concentration. MFBs should be less than ± 30 and ± 60% and MFEs are less than 50 and 75%, respectively, for most concentrations, but they will increase exponentially as concentration decreases below ~ 3 μg m⁻³.

The process of verifying the model results was done by implementation of the Unified Post-Processor (UPP) developed at NOAA and the Model Evaluation Tools (MET) (García-Reynoso and Mora-Ramírez 2017).

Results and discussions

Meteorological variable evaluation

The temporal correlations at all sites in January (*r* = 0.74–0.90) are significantly higher than those in July (*r* = 0.64–0.65) as shown in Table 2. All simulation meets performance goal (i.e., MB from – 0.1 to – 0.7 °C, MAGE from 1.4–2.1 °C, and IOA from 0.79–0.93) for surface temperature in both January and July 2014 as suggested by US EPA (Emery et al. 2001). Similar results were reported in Permadi et al. (2018) where MB ranged from – 1.9 to 0.7 °C for January–March and from – 0.1 to 2.3 °C for August–October using WRF/CHIMERE model system over Southeast Asia domain. In terms of temporal correlations at CEM stations, the model can have a better performance of temperature in January (*r* = 0.9) than that in July (*r* = 0.65). However, the model underestimated the values more in winter (MB = – 0.7) than those in summer (MB = – 0.4). The IOA of all simulation was over 0.7, which is considered to be good. Temperature RMSE ranges from 1.7 to 2.7 K. The bulk of the RMSE lies in systematic error as the unsystematic error ranges between 1 and 1.5 K (Emery et al. 2001). This systematic underestimation was reported in some previous study that apply the Regional Climate Model Version 3 (RegCM3) to simulate temperature at most of the stations over Vietnam (Phan et al. 2009, 2014; Ngo-Duc et al. 2014). In terms of WRF model performance evaluation, it was conducted comparing 30-year simulations (1961–1990) against three station data (Hanoi, Danang, Hochiminh) for temperature (Raghavan et al. 2016). The paper also reported that all stations exhibit high correlations (*r* = 0.81–0.92); the biases were nearly ± 1 °C; the errors such as MAGE and RMSE were 0.87–1.97 °C and 1.71–2.63 °C, respectively. Compared with this study, a greater number of stations (in total 48 stations over Northern Vietnam) were used for the validation, but the time period was more limited. The smaller MB and lower correlation at NCHMF stations than those at CEM stations are also shown. It may be due to

Table 2 Statistical measures calculated for model simulations for meteorological variables

| Simulated time | Jan 2014 | | July 2014 | |
|--------------------|--------------------|--------|--------------------|--------|
| | NCHMF | CEM | NCHMF | CEM |
| Observed time | At 13:00 every day | Hourly | At 13:00 every day | Hourly |
| Number of stations | 45 | 3 | 45 | 3 |
| Temperature | | | | |
| Counts | 900 | 1141 | 855 | 1389 |
| r | 0.74 | 0.90 | 0.64 | 0.65 |
| MB | -0.4 | -0.7 | -0.1 | -0.4 |
| MAGE | 2.0 | 1.4 | 2.1 | 1.6 |
| RMSE | 2.5 | 1.7 | 2.7 | 2.1 |
| IOA | 0.85 | 0.93 | 0.80 | 0.79 |
| Relative humidity | | | | |
| Counts | 900 | 1441 | 855 | 1389 |
| r | 0.74 | 0.72 | 0.34 | 0.60 |
| MB | -11.1 | -8.7 | -2.0 | 1.9 |
| MAGE | 13.2 | 13.7 | 9.6 | 7.9 |
| RMSE | 16.2 | 17.5 | 12.2 | 10.0 |
| IOA | 0.77 | 0.80 | 0.61 | 0.76 |

the discrete data (at 13:00 per day) at NCHMF stations compared with continuous data at CEM stations.

Figure S1 depicts the time series between modeled and observed temperature at three CEM stations in January and July 2014. The model captures diurnal trends of temperature at Hanoi and Phutho but it shows limitation at Quangninh. It is clearly seen that WRF-Chem could not simulate steeply temperature variation in a short time, such as at Quangninh station. The figure shows a reasonable agreement with observation data during the daytime. However, the model seemed to underestimate the temperature during nighttime for both simulation for January and July 2014.

In order to clarify the area that the modeled temperature calculated well, maps of MAGE of all stations in January and July are described in Fig. S2. We divided these into 4 groups by color for representation of MAGE < 2 in January and July (red), MAGE > 2 in January (yellow), MAGE > 2 in July (light blue), and MAGE > 2 in both January and July (purple). MAGE should be smaller than two if the temperature is considered to be replicated well. Overall, there is no clear rule for spatial distribution of MAGE for temperature simulation in January and July. Most of the stations that meet the model performance of MAGE in both January and July (red) were located in the B1 sub-region (Northwest region), while most of the stations that did not meet performance of MAGE in 2 months (purples) were B2 sub-region (Northeast region). We found that the purple dots are over or close to mountain areas, meaning temperature may be strongly influenced by elevation. Thus, we suggest that these errors are likely due

to differences between model topography and the actual height of surface stations (Phan et al. 2009; Ho et al. 2011).

Statistical performance evaluation for hourly relative humidity is described in Table 2. Generally, model predictions agreed well with observation ($r > 0.6$, except for NCHMF in July). In terms of bias and error, the model can replicate the observed humidity in July (i.e., MBs are from -2.0 to 1.9% and MAGEs are from 7.9 to 9.6%, which meet the benchmark values for relative humidity). However, the model significantly underestimated the relative humidity in January (MB = -11.1 to -8.7%; MAGE = 13.2–13.7%) and does not meet the benchmark values. The RMSE averages are from 16.2–17.5% and 10.0–12.2% during January and July, respectively. The IOAs, lower than those of temperature, range within 0.61–0.8 and still meet benchmark values for relative humidity (Emery et al. 2001).

Time series between modeled and observed surface relative humidity at three CEM stations in January and July 2014 are shown in Fig. S3. Surface relative humidity was estimated inconsistently for three stations. It was higher during night time when the temperature decreases. The model seemed to capture the diurnal variation of relative humidity in January. A higher correlation between predicted humidity and observed data was recorded at Hanoi ($r = 0.84$ and 0.63 in January and July, respectively). The agreement was highly remained ($r > 0.7$ in January and July) for Phutho. However, a lower agreement ($r = 0.73$ and 0.48 in January and July) was observed at Quangninh station which is located near the seaside. It could be explained that the humidity was affected by the sea-land

breeze to bring the water vapor from the sea inland and then, resulted in the fluctuations. The results were consistent with Huy (2015) that utilized WRF-CAMx for air quality modeling in Vietnam.

Maps of MAGE for surface relative humidity simulation at 45 NCHMF and 3 CEM stations are presented in Fig. S4. Overall, the model reproduced high accuracy for areas with high surface relative humidity as suggested by simulation in July 2014. However, there are only 7/45 stations which met performance goals with MAGE ($< 10\%$) in both seasons that mainly located closely to seaside. A large number of stations, whose relative humidity are varied within low range in winter (i.e., January), are located in the central mainland area. Unfortunately, there is no previous work that validates simulated data using mesoscale weather forecast model against ground-based data for relative humidity over Vietnam to make any comparison.

We compared our findings with another performance evaluation of WRF-Chem model including nearby Asian region including Oceanic regions. It reported that a comparison between model-simulated and measured meteorological parameters shows only small mean biases and moderate agreements, such as $-0.6\text{ }^{\circ}\text{C}$, $r = 0.36$ in temperature and -1.1% , $r = 0.6$ in relative humidity based on simulation over Bay of Bengal for the summer monsoon season of 2009 (Girach et al. 2017).

Although the meteorology performance for surface temperature and relative humidity does not meet strictly benchmark values for all stations in both months, the results are comparable with other studies and reflect WRF-Chem current ability in reproducing the observed meteorological variables. The difference between observed and modeled data may be explained that local meteorological variables (temperature, relative humidity) were not resolved well at the current horizontal resolution. Local process, e.g., deep convection, is difficult to simulate using the regional model of WRF with the current resolution. The finer resolutions are required to capture the dynamic process happening on smaller scales (Permadi et al. 2018). In addition, it should be noted that these biases may be relative to the observation dataset, such as NCHMF data are only being available at 13:00 or errors in measurement data. Otherwise, a difference is also expected because the model provided a grid average value, while the observation is point value based on individual stations.

PM₁₀ and PM_{2.5} concentration evaluation

The statistical evaluations for modeled daily PM₁₀ and PM_{2.5} concentrations against the observations are described in Table 3. Overall, average model–measurement correlation for average daily PM₁₀ in January ($r = 0.36$) and in July ($r = 0.37$) are similar for all sites. The 24-h average PM_{2.5} concentrations are also consistently in agreement with that in January ($r = 0.59$) and in July ($r = 0.57$). About bias, MFB for 24-h

average PM₁₀ and PM_{2.5} concentration in July (MFB = -27.1 and -40.2 , respectively) is significantly smaller than those in January (MFB = -61.2 and -66.1). Otherwise, MFE has reached closely the performance criteria for PM₁₀ and PM_{2.5} simulation in January (MFE = 63.8 and 66.3) and in July (MFE = 83.9 and 74.9). According to the model performance goals and criteria of PM suggested by Boylan and Russell (2006), the model meets the performance criteria of MFB for all sites with PM_{2.5} simulation in July 2014 but just closely meets criteria in January 2014. About error, MFE satisfied with the performance criteria in simulation of PM₁₀ in January and PM_{2.5} in both January and July 2014.

The correlation coefficient between observed PM₁₀ and PM_{2.5} levels at individual site and modeled values in January ($r = 0.18$ – 0.84 and $r = 0.35$ – 0.75 , respectively) are higher than in July ($r = 0.02$ – 0.06 and $r = -0.03$ – $+0.04$). Both simulations meet the performance criteria (MFB = -53.2 to -27.6 and MFE = 34.8–53.2) for PM₁₀ and PM_{2.5} concentration at Hanoi and Phutho stations, but Quangninh station (MFB = -118.9 to -110.8 and MFE = 110.8–118.9). It is noted that the model can capture reasonable day-by-day variation but with the discrepancy in the range of modeled and observed 24-h PM₁₀, PM_{2.5} is still remarkable. Some previous research has suggested that poor PM predictive performance in winter is common among CTMs and may be attributable to difficulty in reproducing the strongly stable or stagnant weather conditions that are responsible for high winter PM concentrations (Solazzo et al. 2012; Tessum et al. 2015; Zhong et al. 2016). However, this work emphasized that the temporal trend of PM concentration in the wintertime was reproduced well, although the model tends to underestimate and has large negative bias.

According to Kumar et al. (2016), MFBs were -46.19 and -77.07 for 24-h average PM₁₀ using global EDGAR emission inventory with RADM2 and CMBZ mechanism at all stations over Bogota (Kumar et al. 2016) compared with MFB which were between -61.2 (January) and -27.1 (July) in this study. The average coefficient of correlation ($r = 0.38$) for PM₁₀ concentration simulation by applying WRF-Chem in East and South Asia in 4 months in 2007 (Zhong et al. 2016) was similar to our result ($r = 0.36$). However, MFBs were -3.85 to -47.89 and MFEs were 38.05–75.07 also reporting lower in some parts than those in the study (MFB = -27.9 to -118.9 and MFE = 35.7–118.9). Although anthropogenic emission in this study also based on data from REAS (Kurokawa et al. 2013) as Zhong et al. 2016, the MFB and MFE over Vietnam were remarkably high in some parts, Halong station as an example. It is also implied that bottom-up emission inventory, especially high resolution and updated emission data in urban areas (roads or industries) in Vietnam are needed to reduce uncertainties in modeling atmospheric compositions.

Table 3 Statistical evaluation of 24-h average PM₁₀ and PM_{2.5} concentration

| | Station | Count | January 2014 | | | | July 2014 | | | | |
|--|-----------|-------|--------------|---------|---------|---------------------------|-----------|----------|---------|---------|---------------------------|
| | | | <i>r</i> | MFB (%) | MFE (%) | RMSE (µg/m ³) | Count | <i>r</i> | MFB (%) | MFE (%) | RMSE (µg/m ³) |
| PM ₁₀ (µg/m ³) | Quangninh | 19 | 0.8s4 | - 118.9 | 118.9 | 90.5 | 17 | 0.02 | - 115.7 | 115.7 | 18.5 |
| | Hanoi | 19 | 0.67 | - 36.8 | 36.8 | 45.4 | 20 | 0.06 | 48.3 | 56.8 | 26.7 |
| | Phutho | 19 | 0.18 | - 27.9 | 35.7 | 50.8 | - | - | - | - | - |
| | All sites | 57 | 0.36 | - 61.2 | 63.8 | 65.4 | 37 | 0.37 | - 27.1 | 83.9 | 23.3 |
| PM _{2.5} (µg/m ³) | Quangninh | 19 | 0.75 | - 110.8 | 110.8 | 53.7 | 17 | 0.04 | - 115.1 | 117.7 | 10.5 |
| | Hanoi | 19 | 0.60 | - 53.2 | 53.2 | 45.9 | 20 | -0.03 | 23.4 | 38.5 | 13.5 |
| | Phutho | 19 | 0.35 | - 34.2 | 34.8 | 35.5 | - | - | - | - | - |
| | All sites | 57 | 0.59 | - 66.1 | 66.3 | 45.6 | 37 | 0.57 | - 40.2 | 74.9 | 12.2 |

Note: Values in italics represent satisfactory model output. Criteria for MFB $\leq \pm 60\%$ and MFE $\leq 75\%$

Time series of 24-h average concentration of PM₁₀ and PM_{2.5} for January and July is shown in Fig. 2a, b, respectively. Overall, the model seemed to reasonably reproduce PM₁₀ and PM_{2.5} levels in January, during which high levels were found. In other words, the model is difficult to simulate PM₁₀ and PM_{2.5} at low range in July. Additionally, the model underestimated PM₁₀ and PM_{2.5} levels of all simulations for all sites (except simulation for Hanoi in July). In Quangninh, the modeled 24-h average PM₁₀ was 3–65 µg m⁻³ as compared with the observed range of 13–173 µg m⁻³. In the urban station in Hanoi close to a busy road, the simulated 24-h average PM₁₀ was 38–136 µg m⁻³ as compared with the observed range of 14–174 µg m⁻³. In Phutho site, modeled 24-h average PM₁₀ was within range of 64–140 µg m⁻³ while the observed was 74–192 µg m⁻³. Similarly, the modeled underestimated observed PM_{2.5} values range from 2 to 48 µg m⁻³ at the station in Quangninh, while the range fluctuated from 7 to 107 µg m⁻³. For Hanoi, the modeled values were from 22 to 92 µg m⁻³ while the observed values were 12–133 µg m⁻³. However, both sites showed linear correlation in January, but lower correlation in July. A better agreement in the range of 24-h PM_{2.5} levels was found at Phutho station in January. There was a lack of observation data in July at Phutho station. The modeled 24-h PM_{2.5} concentrations were ranged within 45–99 µg m⁻³, but observed concentrations were from around 51 µg m⁻³ to 130 µg m⁻³ at this site.

WRF-Chem could generally reproduce well temporal variation of PM concentration at Quangninh and Hanoi stations, but not at the Phutho site. It could be linked to the local meteorological variables that were not resolved well at the current horizontal resolution as mentioned above. The explanation was also supported by Min et al. (2016) in which PM₁₀ simulation was utilized by WRF-Chem over East Asia (Zhong et al. 2016). On the other hand, MFB and MFE in PM₁₀ and PM_{2.5} simulation against observation data at Phutho station nearly reached

the performance goal. The discrepancy in the day-to-day variation between the modeled and observed PM could be attributed to the lower accuracy of the temporal variations of the emission input data as suggested by (Permadi et al. 2018). Furthermore, the baseline year of the emission inventory used in this paper is 2010, which is 4 years lagged. The changes in emission from 2010 to 2014 may be due to changing economic activity. The level of development and the control of air pollutant emitting were much different from each other in this region. The usage of the emission is involving large uncertainty, which may be much different from emission species. Thus, uncertainty was brought into results due to annual lagging. Other factors may be caused by meteorological input data. Otherwise, the uncertainty could come from secondary aerosol formation that GOCART scheme did not estimate. For example, the percentage of secondary aerosol mix accounted for 40% of total mass PM_{2.5} concentration was reported by Hai and Kim Oanh (2013). In addition, lack of monitoring data in rural sites and a large number of missing data prevented us from making sufficient model performance evaluation, both for the PM mass concentrations and their ratios. Further studies in the future are needed to address these issues.

Spatial distribution of PM₁₀ and PM_{2.5} concentrations

Spatial distribution of the average monthly modeled PM₁₀ and PM_{2.5} mass concentration for January and July 2014 is illustrated in Fig. 3a–d, respectively. Overall, the average monthly of coarse and fine PM were higher in January (17–111 µg m⁻³ for PM₁₀ and 12–73 µg m⁻³ for PM_{2.5}) than those in July (1–70 µg m⁻³ for PM₁₀ and 1–37 µg m⁻³ for PM_{2.5}). This seasonal variation was also similar in several Asian regions including Vietnam, which indicates the regional contribution to PM_{2.5} levels (Cohen et al. 2002; Ly et al. 2018). These figures

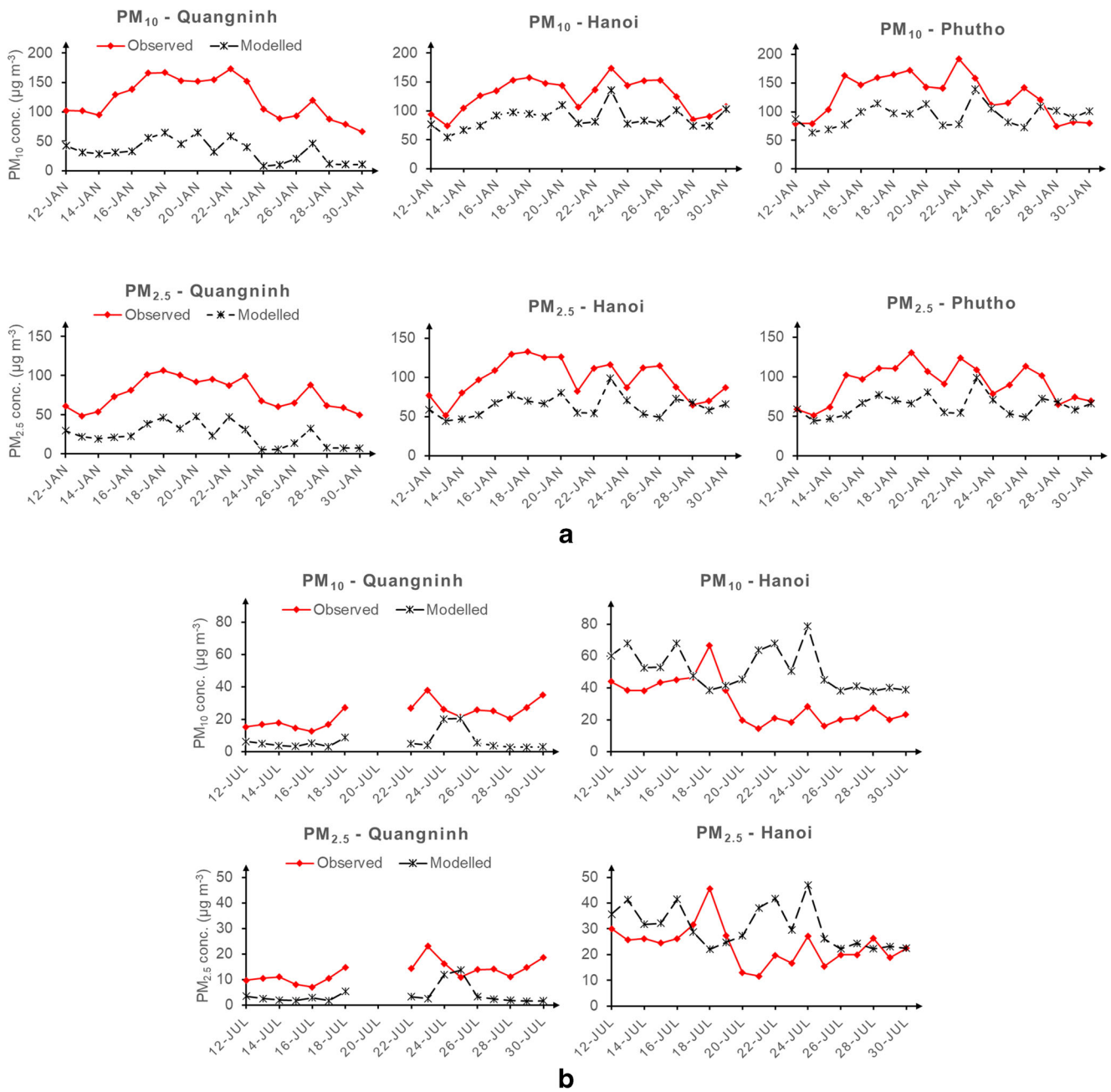


Fig. 2 Time series of modeled and observed PM_{10} and $PM_{2.5}$ at Quangninh, Hanoi, and Phu Tho stations in January (a) and Quangninh and Hanoi stations in July (b) 2014

also saw that the highest concentrations of both PM_{10} (above $80 \mu\text{g m}^{-3}$ in January and around $50 \mu\text{g m}^{-3}$ in July) and $PM_{2.5}$ (above $50 \mu\text{g m}^{-3}$ in January and $30 \mu\text{g m}^{-3}$ in July) were found over Hanoi cities and nearby satellite cities where traffic and residential emission were considered as dominant emission sources. On the other hand, the lowest of those were observed in the mountainous area where PM_{10} was roughly under $30 \mu\text{g m}^{-3}$ and $PM_{2.5}$ was less than $20 \mu\text{g m}^{-3}$ in January. High-concentration areas were found to be larger in July than in January. As a result, the model seemed to capture

reasonably spatial variation of both coarse and fine particle concentrations in conjunction with seasonal variation.

$PM_{2.5}/PM_{10}$ ratio

$PM_{2.5}$ mass is principally contributed by both local combustion sources and secondary particle formation by chemical reactions in the atmosphere. The gaseous precursors of NO_x , SO_x , and VOCs for the $PM_{2.5}$ formation may have both local and LRT origins (Permadi et al. 2018). The coarse fraction

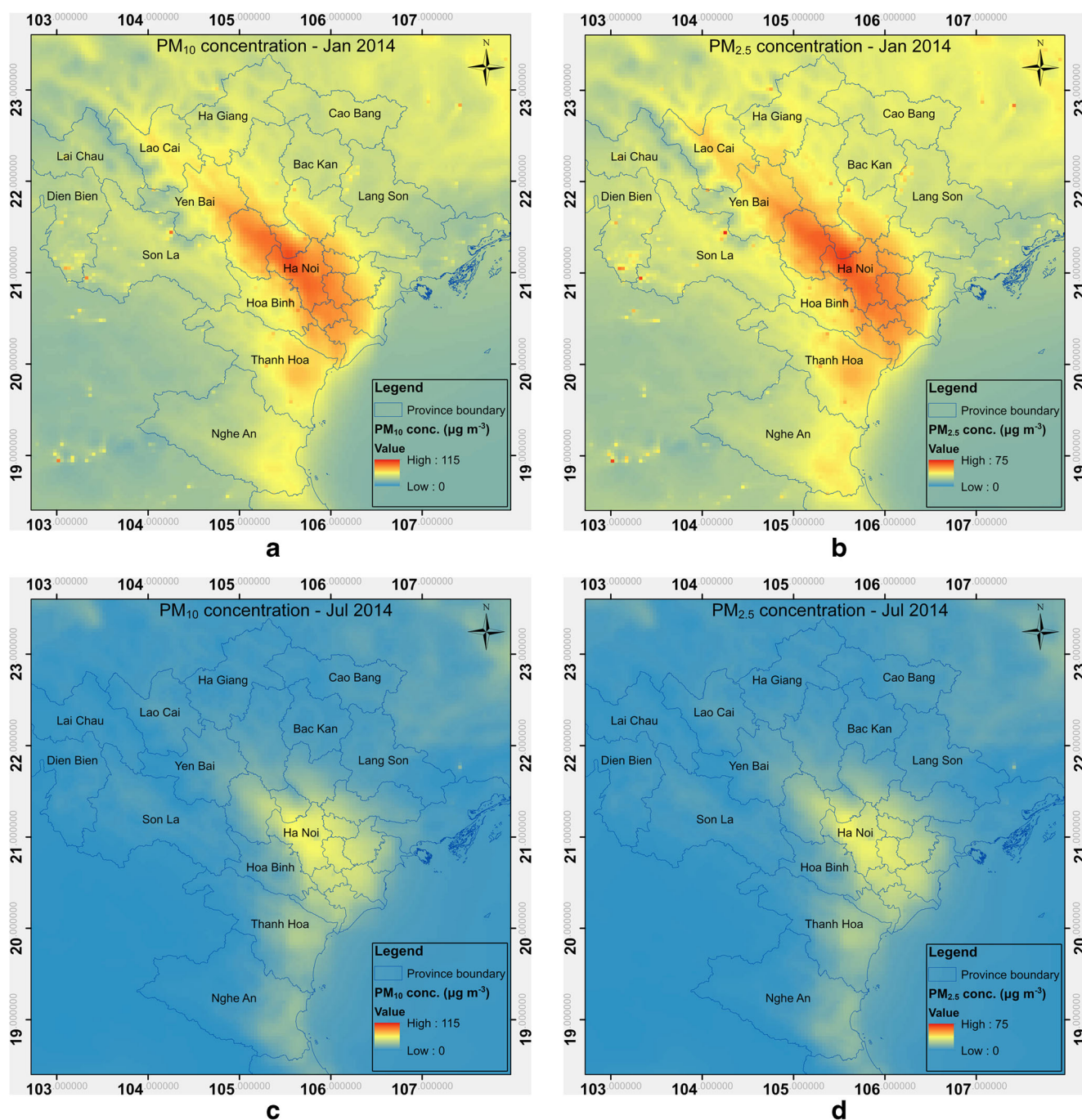


Fig. 3 Spatial distribution of average monthly PM_{10} and $PM_{2.5}$ concentrations ($\mu\text{g m}^{-3}$) in January (a, b) and July (c, d) 2014

($PM_{10-2.5}$) would mainly consist of primary particles of the geological origin (Chow et al. 1998) and local sources of soil, road dust, and construction activities (Hai and Kim Oanh 2013). The $PM_{2.5}/PM_{10}$ ratios could support to determine the dominance of local sources of $PM_{2.5}$. $PM_{2.5}/PM_{10}$ ratios were calculated based on the modeled 24-h values and those computed from the observed PM data available at the three CEM monitoring sites. Table 4 shows a comparison of $PM_{2.5}/PM_{10}$ ratios between WRF-Chem simulation and observation in January and July 2014 at each site. Overall, the modeled

$PM_{2.5}/PM_{10}$ ratios ranged from 0.58 to 0.69 while the observed values were higher, 0.57–0.82. Greater ratio differences were observed at Hanoi station, 0.79 vs. 0.62, and at Phutho station, 0.73 vs. 0.68 for observation and modeling, respectively. Better agreements were obtained at Quangninh station, observed at 0.60 vs. modeled at 0.63. Higher $PM_{2.5}/PM_{10}$ ratios during the dry season as compared to the wet season may be attributed to higher fossil fuel combustion emission, more secondary particle formation due to more intensive photochemical reactions (Kim Oanh et al. 2006). The

Table 4 Comparison of PM_{2.5}/PM₁₀ ratio from WRF-Chem simulation and observation

| Station | Quangninh | | Hanoi | | Phutho | |
|---------|-------------|----------|-------------|----------|-------------|----------|
| | Observation | Modeling | Observation | Modeling | Observation | Modeling |
| January | 0.64 | 0.69 | 0.76 | 0.64 | 0.73 | 0.68 |
| July | 0.57 | 0.58 | 0.82 | 0.59 | - | - |
| Average | 0.60 | 0.63 | 0.79 | 0.62 | 0.73 | 0.68 |

results highlighted that the ratios of the model-simulated PM_{2.5}/PM₁₀ were acceptable at Quangninh and Phutho stations, but not at Hanoi station; this would imply a necessity of further improvement of PM speciation of the emission input data.

Assessment of the effects of biomass burning emission

Biomass burning after harvesting episodes in some parts of Vietnam was reported to contribute to air pollution in some previous studies (Le et al. 2014; Kim Oanh et al. 2018; Nhu Ngoc et al. 2018). Intensive biomass burning episodes in northern Vietnam usually occur in two episodes, the first one lasts from end of May to middle of June and the later occurs in October–November. However, the stagnant weather conditions in the winter also were one of the reasons which caused the air quality deterioration suggested by Hien et al. (2002). Thus, preliminary assessment of the influence of biomass burning emission on air quality over northern Vietnam was conducted in the period of May–June 2014 to eliminate influence of the bad weather conditions.

Figure 4 shows day-by-day variation between active fires and average PM₁₀ and PM_{2.5} levels in May–June 2014 for over the inner domain d03. Active fires were counted from VIIRS fire products and precipitation was obtained from WRF-Chem outputs. It can be seen that some peaks of PM₁₀ and PM_{2.5} were observed when burning activities were intensive (i.e., large number of fires).

For instance, the 24-h average concentration of PM₁₀ and PM_{2.5} reached the highest point (32 µg m⁻³ and 22 µg m⁻³, respectively) and the number of fires was 376 based on VIIRS images on 15 May. Similarly, the phenomenon was repeated also on several days (11th–12th, 14th, 22nd–25th of May, 2nd–6th of June). On 10 May, there is an inverse correlation between fire counts and PM₁₀ and PM_{2.5} concentrations; it may be due to fire emission needing time to affect and wet removal occurred, in other words, the peak concentration was observed the day after. For example, the PM₁₀ and PM_{2.5} concentrations declined following the increasing precipitation on the 19th–21st of May (10–15 mm) and 5th–10th of June (25–30 mm). In turn, a lower fire count was found on some days with high precipitation (i.e., 5th–9th and 27th–29th of May, 4th–14th of June). There was a moderate correlation between precipitation and PM₁₀ and PM_{2.5} concentrations ($r = -0.59$, not showed) and there was an inverse correlation between precipitation and biomass burning emission ($r = -0.44$, not showed). It should be noted that biomass burning emission had negative influence while precipitation had positive effects on PM_{2.5} and PM₁₀ concentrations in this period.

A scatter plot between total hotspots and daily PM₁₀ and PM_{2.5} concentration is presented in Fig. 5. It reveals that there was a moderate day-by-day correlation between biomass burning and PM₁₀ and PM_{2.5} concentrations; coefficients of determination (R^2) were 0.53 and 0.49, respectively, over the study area. Similar results ($R^2 = 0.2–0.6$) were given by (Punsompong and Chantara 2018) that identify the potential

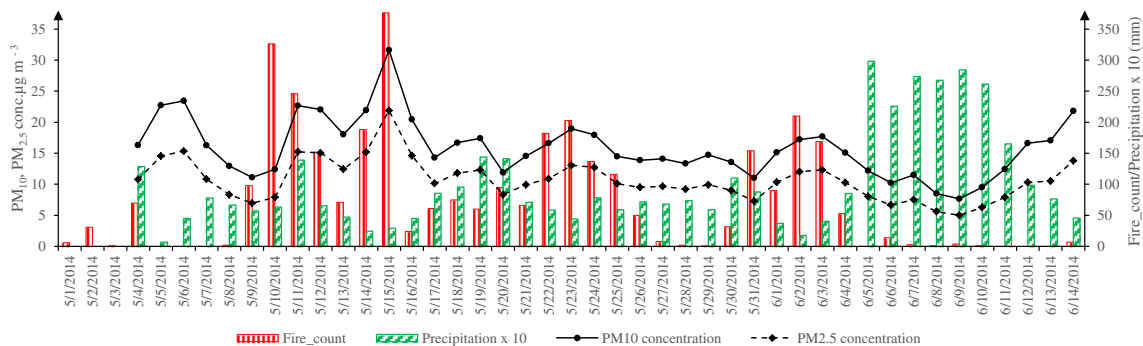
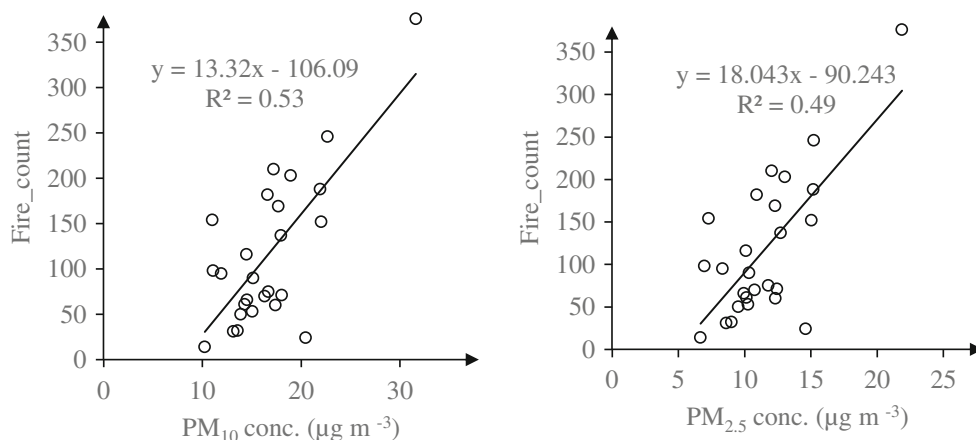


Fig. 4 Time series of total hotspots and precipitation corresponding to average 24-h PM₁₀ and PM_{2.5} concentrations

Fig. 5 Correlation between daily total hotspots and average 24-h PM_{10} (left) and $PM_{2.5}$ concentrations (right)



effects of biomass burning in Thailand. Another study explored the influence of biomass burning on aerosol over Southern Vietnam. The authors showed that correlation between aerosol optical depth aerosol and fire counts based on Moderate Resolution Imaging Spectroradiometer (MODIS) was weak ($R^2 = 0.1$). They also reported that the correlations in forest, plantation, and peat land fires were relatively higher than the agricultural fires (Vadrevu et al. 2015). Thus, the weak correlation could be coming from the uncertainty in detecting fires because the agricultural fires are dominant in this study area and 1-km pixel-by-pixel validation. Besides, these results implied that the concentration of PM_{10} and $PM_{2.5}$ in this area may be affected by other sources, such as vehicle emissions or cooking more than biomass burning sources (Hai and Kim Oanh 2013). Further PM composition analyzing should be done to make an in-depth assessment of biomass burning as well as other sources on air quality.

Spatial distribution of monthly average PM_{10} and $PM_{2.5}$ are presented in Fig. S5 for May–June 2014. The highest monthly average PM_{10} concentration for the whole domain was $100 \mu g m^{-3}$ while corresponding value of $PM_{2.5}$ was $77 \mu g m^{-3}$.

Larger hotspots with lower concentration around $60 \mu g m^{-3}$ for PM_{10} and approximately $35 \mu g m^{-3}$ for $PM_{2.5}$ were observed over Red River Delta, which can be explained by the influence of emission from residential areas and traffic in Hanoi city and surrounding areas. Especially, higher concentrations (above $70 \mu g m^{-3}$ for PM_{10} concentration and above $40 \mu g m^{-3}$ for $PM_{2.5}$) were found at fragmented places which active fires were in high-frequency occurrences (see Fig. S6). In comparison with simulation of PM concentration for January and July (see Fig. 3), some observed high values should be corresponding to fire hotspots.

The contribution of crop residue burning to surface PM_{10} and $PM_{2.5}$ concentration was calculated by subtracting the model result of EXP_NOFINN (experiment without FINN) from those of EXP_FINN (experiment with FINN). The

spatial distribution of the different concentrations of PM_{10} and $PM_{2.5}$ between with and without biomass burning emission is showed in Fig. 6.

The figure showed that the concentration of PM_{10} and $PM_{2.5}$ contributing from biomass burning within range -12 to $+90 \mu g m^{-3}$ and -9 to $+76 \mu g m^{-3}$, respectively. The most significant difference in which a great number of fire count points, for example parts of Nghean, Quangninh, and intersection areas of Backan, Caobang, and Langson provinces. However, there is not much difference in PM concentration over Hanoi and surrounding area which traffic and residential emission were dominant. It is also noted that VIIRS satellite could not capture small fires at high resolution, thus we have just assessed biomass burning episode over the whole area. Comprehensive assessment of biomass burning effects on air quality at specific sites is beyond this study.

Conclusions

WRF-Chem online model systems were utilized for meteorology and air quality over northern Vietnam. Simulations were conducted in both of wintertime and summertime to investigate seasonal variation modeling of air quality. The results of validation procedure were found that WRF-Chem can capture seasonal variation of surface meteorological variables and PM mass concentration in the atmosphere. The model meets performance goal suggested by US EPA for surface temperature and relative humidity at 45 NCHMF stations, while it meets performance criteria for PM mass concentration almost at CEM observation sites. WRF-Chem could generally reproduce well the temporal variation of PM concentration at Quangninh and Hanoi stations, but it is limited in reflecting PM concentration variation at Phutho site. However, MFB and MFE of PM_{10} and $PM_{2.5}$ simulation against observation data at Phutho station are nearly reached to performance goal. We suggested that the uncertainty may be mainly caused by

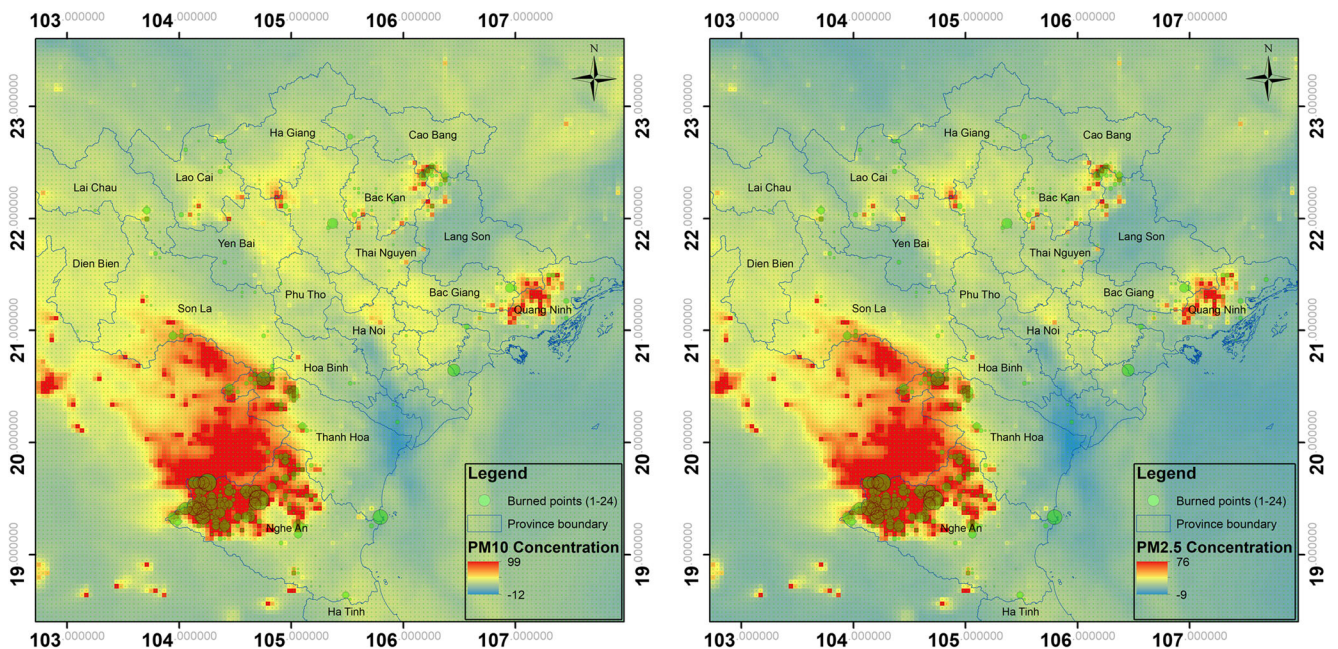


Fig. 6 Spatial distribution of the different concentrations of PM₁₀ (left) and PM_{2.5} (right) between experiment with and without biomass burning emission over the period of 1 May–15 June 2014

the emission input data where local sources and high-resolution data should be updated. Other factors may be causes including meteorological input data or the uncertainty of secondary aerosol formation scheme. Furthermore, monitoring system should be expanded to make comprehensive model performance evaluation for the PM mass concentrations and their components.

We also implemented WRF-Chem to simulate air quality in May–June 2014 when intensive biomass burning occurred over this area. VIIRS satellite datasets were supporting data to observe fire hotspots. PM₁₀ and PM_{2.5} were higher at the time and the area with the larger number of fires was found. The results are consistent with other previous studies stating that biomass burning is one of contributing sources, besides local sources such as traffic or cooking impacts on air quality over the region in summer.

Our results highlight the usefulness of WRF-Chem and satellite remote sensing data in modeling air quality and capturing the pollution events. We advocate the integration of diversity data sources, such as satellite remote sensing data and ground-based observation data in conjunction with assimilation approach in online model system for building innovative operational air quality forecasts in the region to address haze impacts and health concerns.

Acknowledgments We would like to thank the Center for Environmental Monitoring, Vietnam Environmental Agency, for providing measurement air quality data over Vietnam. We are also thankful to the Vietnam National Centre for Hydrometeorological Forecasting for supplying observation meteorological data.

Funding information This research is funded by Vietnam National Foundation for Science and Technology Development (NAFOSTED) under grant number 105.08-2017.11.

References

An DD (2005) Photochemical smog modeling for air quality management in the Hanoi metropolitan region. Vietnam, Asian Institute of Technology, Pathumthani, Thailand

Anderson JO, Thundiyil JG, Stolbach A (2012) Clearing the air: a review of the effects of particulate matter air pollution on human health. *J Med Toxicol* 8:166–175. <https://doi.org/10.1007/s13181-011-0203-1>

Bessagnet B, Menut L, Curd G et al (2008) Regional modeling of carbonaceous aerosols over Europe-focus on secondary organic aerosols. *J Atmos Chem* 61:175–202. <https://doi.org/10.1007/s10874-009-9129-2>

Boylan JW, Russell AG (2006) PM and light extinction model performance metrics, goals, and criteria for three-dimensional air quality models. *Atmos Environ* 40:4946–4959. <https://doi.org/10.1016/j.atmosenv.2005.09.087>

Chow JC, Watson JG, Lowenthal DH, Egami RT, Solomon PA, Thuillier RH, Magliano K, Ranzieri A (1998) Spatial and temporal variations of particulate precursor gases and photochemical reaction products during SJVAQS/AUSPEX ozone episodes. *Atmos Environ* 32: 2835–2844. [https://doi.org/10.1016/S1352-2310\(97\)00449-4](https://doi.org/10.1016/S1352-2310(97)00449-4)

Collett RS, Oduyemi K (1997) Air quality modelling: a technical review of mathematical approaches. *Meteorol Appl* 4:235–246. <https://doi.org/10.1017/S1350482797000455>

Danh NT, Huy LN, Oanh NTK (2016) Assessment of rice yield loss due to exposure to ozone pollution in Southern Vietnam. *Sci Total Environ* 566–567:1069–1079. <https://doi.org/10.1016/j.scitotenv.2016.05.131>

- de Almeida Albuquerque TT, de Fátima AM, Ynoue RY et al (2018) WRF-SMOKE-CMAQ modeling system for air quality evaluation in São Paulo megacity with a 2008 experimental campaign data. *Environ Sci Pollut Res* 25:36555–36569. <https://doi.org/10.1007/s11356-018-3583-9>
- Emery C, Tai E, Yarwood G (2001) Enhanced meteorological modeling and performance evaluation for two Texas ozone episodes. Prepared for the Texas Natural Resource Conservation Commission (now TCEQ), by ENVIRON International Corp, Novato, CA. <https://www.tceq.texas.gov/assets/public/implementation/air/am/contracts/reports/mm/EnhancedMetModelingAndPerformanceEvaluation.pdf>
- Emmons LK, Walters S, Hess PG, Lamarque JF, Pfister GG, Fillmore D, Granier C, Guenther A, Kinnison D, Laepple T, Orlando J, Tie X, Tyndall G, Wiedinmyer C, Baughcum SL, Kloster S (2010) Description and evaluation of the Model for Ozone and Related chemical Tracers, version 4 (MOZART-4). *Geosci Model Dev* 3: 43–67. <https://doi.org/10.5194/gmd-3-43-2010>
- Fast JD, Gustafson WI, Easter RC, et al (2006) Evolution of ozone, particulates, and aerosol direct radiative forcing in the vicinity of Houston using a fully coupled meteorology-chemistry-aerosol model. *J Geophys Res-Atmos* 111:1–29. <https://doi.org/10.1029/2005JD006721>
- Ferretti M, Andrei S, Caldini G, Grechi D, Mazzali C, Galanti E, Pellegrini M (2008) Integrating monitoring networks to obtain estimates of ground-level ozone concentrations - a proof of concept in Tuscany (central Italy). *Sci Total Environ* 396:180–192. <https://doi.org/10.1016/j.scitotenv.2008.02.019>
- García-Reynoso A, Mora-Ramírez MA (2017) Implementation of the Unified Post Processor (UPP) and the Model Evaluation Tools (MET) for WRF-chem evaluation performance. *Atmosfera* 30: 259–273. <https://doi.org/10.20937/ATM.2017.30.03.06>
- Georgiou GK, Christoudias T, Proestos Y, Kushta J, Hadjinicolaou P, Lelieveld J (2018) Air quality modelling in the summer over the eastern Mediterranean using WRF/Chem: chemistry and aerosol mechanisms intercomparison. *Atmos Chem Phys* 18:1555–1571. <https://doi.org/10.5194/acp-18-1555-2018>
- Girach IA, Ojha N, Nair PR, Pozzer A, et al (2017) Variations in O₃, CO, and CH₄ over the Bay of Bengal during the summer monsoon season: shipborne measurements and model simulations. *Atmos Chem Phys* 17:257–275. <https://doi.org/10.5194/acp-17-257-2017>
- González CM, Ynoue RY, Vara-Vela A et al (2018) High-resolution air quality modeling in a medium-sized city in the tropical Andes: assessment of local and global emissions in understanding ozone and PM₁₀ dynamics. *Atmos Pollut Res* 0–1. <https://doi.org/10.1016/j.apr.2018.03.003>
- Grell G, Baklanov A (2011) Integrated modeling for forecasting weather and air quality: a call for fully coupled approaches. *Atmos Environ* 45:6845–6851. <https://doi.org/10.1016/j.atmosenv.2011.01.017>
- Grell GA, Peckham SE, Schmitz R, McKeen SA, Frost G, Skamarock WC, Eder B (2005) Fully coupled “online” chemistry within the WRF model. *Atmos Environ* 39:6957–6975. <https://doi.org/10.1016/j.atmosenv.2005.04.027>
- Guenther AB, Jiang X, Heald CL, Sakulyanontvittaya T, Duhl T, Emmons LK, Wang X (2012) The model of emissions of gases and aerosols from nature version 2.1 (MEGAN2.1): an extended and updated framework for modeling biogenic emissions. *Geosci Model Dev* 5:1471–1492. <https://doi.org/10.5194/gmd-5-1471-2012>
- Hai CD, Kim Oanh NT (2013) Effects of local, regional meteorology and emission sources on mass and compositions of particulate matter in Hanoi. *Atmos Environ* 78:105–112. <https://doi.org/10.1016/j.atmosenv.2012.05.006>
- Hien PD, Bac VT, Tham HC, Nhan DD, Vinh LD (2002) Influence of meteorological conditions on PM_{2.5} and PM_{2.5-10} concentrations during the monsoon season in Hanoi, Vietnam. *Atmos Environ* 36: 3473–3484. [https://doi.org/10.1016/S1352-2310\(02\)00295-9](https://doi.org/10.1016/S1352-2310(02)00295-9)
- Cohen DD, Garton D, Stelcer E, Wang T, Poon S, Kim J et al (2002) Characterization of PM_{2.5} and PM₁₀ fine particle pollution in several Asian regions, 16th Int. Clean Air Conf. Christchurch, NZ, 18–22 Aug 02
- Ho BQ (2017) Modeling PM₁₀ in Ho Chi Minh City, Vietnam and evaluation of its impact on human health. *Sustain Environ Res* 27: 95–102. <https://doi.org/10.1016/j.serj.2017.01.001>
- Ho TMH, Phan VT, Le NQ, Nguyen QT (2011) Extreme climatic events over Vietnam from observational data and RegCM3 projections. *Clim Res* 49:87–100. <https://doi.org/10.3354/cr01021>
- Huy LN (2015) Evaluation of performance of photochemical smog modeling system for air quality management in Vietnam. Asian Institute of Technology, Pathumthani, Thailand
- IPCC (2013) Climate change 2013 - the physical science basis: summary for policymakers, technical summary and frequently asked questions. Intergovernmental Panel on Climate Change 222. <https://doi.org/10.1038/446727a>
- Janssens-Maenhout G, Crippa M, Guizzardi D, Dentener F, Muntean M, Pouliot G, Keating T, Zhang Q, Kurokawa J, Wankmüller R, Denier van der Gon H, Kuenen JJP, Klimont Z, Frost G, Darras S, Koffi B, Li M (2015) HTAP-v2.2: a mosaic of regional and global emission grid maps for 2008 and 2010 to study hemispheric transport of air pollution. *Atmos Chem Phys* 15:11411–11432. <https://doi.org/10.5194/acp-15-11411-2015>
- Kim Oanh NT, Upadhyay N, Zhuang YH, Hao ZP, Murthy DVS, Lestari P, Villarin JT, Chengchua K, Co HX, Dung NT (2006) Particulate air pollution in six Asian cities: spatial and temporal distributions, and associated sources. *Atmos Environ* 40:3367–3380. <https://doi.org/10.1016/j.atmosenv.2006.01.050>
- Kim Oanh NT, Permadi DA, Hopke PK, Smith KR, Dong NP, Dang AN (2018) Annual emissions of air toxics emitted from crop residue open burning in Southeast Asia over the period of 2010–2015. *Atmos Environ* 187:163–173. <https://doi.org/10.1016/j.atmosenv.2018.05.061>
- Kumar R, Naja M, Pfister GG, Barth MC, Wiedinmyer C, Brasseur GP (2012) Simulations over South Asia using the Weather Research and Forecasting model with Chemistry (WRF-Chem): chemistry evaluation and initial results. *Geosci Model Dev* 5:619–648. <https://doi.org/10.5194/gmd-5-619-2012>
- Kumar A, Jiménez R, Belalcázar LC, Rojas NY (2016) Application of WRF-chem model to simulate PM₁₀ concentration over Bogota. *Aerosol Air Qual Res* 16:1206–1221. <https://doi.org/10.4209/aaqr.2015.05.0318>
- Kurokawa J, Ohara T, Morikawa T, Hanayama S, Janssens-Maenhout G, Fukui T, Kawashima K, Akimoto H (2013) Emissions of air pollutants and greenhouse gases over Asian regions during 2000–2008: Regional Emission inventory in ASia (REAS) version 2. *Atmos Chem Phys* 13:11019–11058. <https://doi.org/10.5194/acp-13-11019-2013>
- Le TH, Nguyen TNT, Lasko K et al (2014) Vegetation fires and air pollution in Vietnam. *Environ Pollut* 195:267–275. <https://doi.org/10.1016/j.envpol.2014.07.023>
- Ly BT, Matsumi Y, Nakayama T et al (2018) Characterizing PM_{2.5} in Hanoi with new high temporal resolution sensor. 2487–2497. <https://doi.org/10.4209/aaqr.2017.10.0435>
- Mar KA, Ojha N, Pozzer A, Butler TM (2016) Ozone air quality simulations with WRF-Chem (v3.5.1) over Europe: model evaluation and chemical mechanism comparison. *Geosci Model Dev* 9:3699–3728. <https://doi.org/10.5194/gmd-9-3699-2016>
- Mian C, Richard BR, Shian-Jian L et al (2000) Atmospheric sulfur cycle simulated in the global model GOCART: model description and global properties. *J Geophys Res* 105:24,671–24,687
- MONRE (2016) National State of environment reports (in Vietnamese)

- Mues A, Lauer A, Lupascu A et al (2018) WRF and WRF-Chem v3.5.1 simulations of meteorology and black carbon concentrations in the Kathmandu Valley. *Geosci Model Dev* 11:2067–2091. <https://doi.org/10.1007/978-3-319-24478-5>
- Nghiem LH (2008) Photochemical modeling for simulation of ground-level ozone over the continental Southeast Asian region to assess potential impacts on rice crop. Asian Institute of Technology, Pathumthani, Thailand
- Ngo-Duc T, Kieu C, Thatcher M, Nguyen-le D, Phan-van T (2014) Climate projections for Vietnam based on regional climate models. *Clim Res* 60:199–213. <https://doi.org/10.3354/cr01234>
- Nguyen TNT, Ta VC, Le TH, Mantovani S (2014) Particulate matter concentration estimation from satellite aerosol and meteorological parameters: data-driven approaches. In: Huynh V-N, Dencœur T, Tran DH, et al. (eds) *Advances in intelligent systems and computing*. Springer, pp 351–362
- Nguyen TTN, Bui HQ, Pham HV, Luu HV, Man CD, Pham HN, le HT, Nguyen TT (2015) Particulate matter concentration mapping from MODIS satellite data: a Vietnamese case study. *Environ Res Lett* 10:095016. <https://doi.org/10.1088/1748-9326/10/9/095016>
- Nguyen TNT, Ha DV, Do TNN, Nguyen VH, Ngo XT, Phan VH, Nguyen ND, Bui QH (2019a) Air pollution monitoring network using low-cost sensors, a case study in Hanoi, Vietnam. *IOP Conf Ser Earth Environ Sci* 266:012017. <https://doi.org/10.1088/1755-1315/266/1/012017>
- Nguyen TNT, Le HA, Mac TMT et al (2019b) Current status of PM_{2.5} pollution and its mitigation in Vietnam. *Glob Environ Res* 22:73–83
- Nhu Ngoc DT, Duyen LT, Yusuke S et al (2018) Source apportionment of Vocs by receptor modelling in an urban site in Ha Noi. *Vietnam J Sci Technol* 56:88–95. <https://doi.org/10.15625/2525-2518/56/2c/13034>
- Nopmongcol U, Koo B, Tai E, Jung J, Piyachaturawat P, Emery C, Yarwood G, Pirovano G, Mitsakou C, Kallos G (2012) Modeling Europe with CAMx for the air quality model evaluation international initiative (AQMEII). *Atmos Environ* 53:177–185. <https://doi.org/10.1016/j.atmosenv.2011.11.023>
- Oanh NTK (ed) (2013) *Integrated air quality management - Asian case studies*. CRC Press, Taylor & Francis Group, New York, USA
- Pérez Ballesta P, Field RA, Fernández-Patier R, Galán Madruga D, Connolly R, Baeza Caracena A, de Saeger E (2008) An approach for the evaluation of exposure patterns of urban populations to air pollution. *Atmos Environ* 42:5350–5364. <https://doi.org/10.1016/j.atmosenv.2008.02.047>
- Permadi DA, Kim Oanh NT, Vautard R (2017) Assessment of co-benefits of black carbon emission reduction measures in Southeast Asia: part 1 emission inventory and simulation for the base year 2007. *Atmos Chem Phys Discuss* 1–35. <https://doi.org/10.5194/acp-2017-315>
- Permadi DA, Oanh NTK, Vautard R (2018) Integrated emission inventory and modeling to assess distribution of particulate matter mass and black carbon composition in Southeast Asia. *Atmos Chem Phys* 18:2725–2747. <https://doi.org/10.5194/acp-18-2725-2018>
- Phan V-T, Ngo-Duc T, Ho T-M-H (2009) Seasonal and interannual variations of surface climate elements over Vietnam. *Clim Res* 40:49–60. <https://doi.org/10.3354/cr00824>
- Phan VT, Nguyen VH, Trinh TL et al (2014) Seasonal prediction of surface air temperature across Vietnam using the Regional Climate Model version 4.2 (RegCM4.2). *Adv Meteorol* 2014:1–13. <https://doi.org/10.1155/2014/245104>
- Punsompong P, Chantara S (2018) Identification of potential sources of PM₁₀ pollution from biomass burning in northern Thailand using statistical analysis of trajectories. *Atmos Pollut Res* 0–1. <https://doi.org/10.1016/j.apr.2018.04.003>, 9, 1038
- Raghavan SV, Vu MT, Liong SY (2016) Regional climate simulations over Vietnam using the WRF model. *Theor Appl Climatol* 126:161–182. <https://doi.org/10.1007/s00704-015-1557-0>
- Simpson D, Fagerli H, Jonson JE, et al (2003) Transboundary acidification, eutrophication and ground level ozone in Europe, part I. Unified EMEP model description, EMEP Status Report 1/2003, Norwegian Meteorological Institute, Oslo, 74 p. EMEP Report 1/2003 74
- Solazzo E, Bianconi R, Pirovano G, Matthias V, Vautard R, Moran MD, Wyatt Appel K, Bessagnet B, Brandt J, Christensen JH, Chemel C, Coll I, Ferreira J, Forkel R, Francis XV, Grell G, Grossi P, Hansen AB, Miranda AI, Nopmongcol U, Prank M, Sartelet KN, Schaap M, Silver JD, Sokhi RS, Vira J, Werhahn J, Wolke R, Yarwood G, Zhang J, Rao ST, Galmarini S (2012) Operational model evaluation for particulate matter in Europe and North America in the context of AQMEII. *Atmos Environ* 53:75–92. <https://doi.org/10.1016/j.atmosenv.2012.02.045>
- Stölzel M, Breiter S, Cyrus J, Pitz M, Wölke G, Kreyling W, Heinrich J, Wichmann HE, Peters A (2007) Daily mortality and particulate matter in different size classes in Erfurt, Germany. *J Expo Sci Environ Epidemiol* 17:458–467. <https://doi.org/10.1038/sj.jes.7500538>
- Tessum CW, Hill JD, Marshall JD (2015) Twelve-month, 12 km resolution North American WRF-Chem v3.4 air quality simulation: performance evaluation. *Geosci Model Dev* 8:957–973. <https://doi.org/10.5194/gmd-8-957-2015>
- Tuccella P, Curci G, Visconti G, Bessagnet B, Menut L, Park RJ (2012) Modeling of gas and aerosol with WRF/Chem over Europe: evaluation and sensitivity study. *J Geophys Res-Atmos* 117:1–15. <https://doi.org/10.1029/2011JD016302>
- Vadrevu KP, Lasko K, Giglio L, Justice C (2015) Vegetation fires, absorbing aerosols and smoke plume characteristics in diverse biomass burning regions of Asia. *Environ Res Lett* 10:105003. <https://doi.org/10.1088/1748-9326/10/10/105003>
- Van DTH, Trung NQ, Hiep N Van, Tan P Van (2014) Simulation of aerosol impacts on weather over Vietnam region by WRF/CHEM model. In: Meeting of the consortium of Asian universities in Fukuoka (CAUFUK). Fukuoka, Japan
- Wiedinmyer C, Akagi SK, Yokelson RJ, Emmons LK, al-Saadi JA, Orlando JJ, Soja AJ (2011) The fire INventory from NCAR (FINN): a high resolution global model to estimate the emissions from open burning. *Geosci Model Dev* 4:625–641. <https://doi.org/10.5194/gmd-4-625-2011>
- Yahya K, Wang K, Campbell P, Chen Y, Glotfelty T, He J, Pirhalla M, Zhang Y (2017) Decadal application of WRF/Chem for regional air quality and climate modeling over the U.S. under the representative concentration pathways scenarios. Part 1: model evaluation and impact of downscaling. *Atmos Environ* 152:562–583. <https://doi.org/10.1016/j.atmosenv.2016.12.029>
- Zhang Y (2008) Online-coupled meteorology and chemistry models: history, current status, and outlook. *Atmos Chem Phys* 8:2895–2932. <https://doi.org/10.5194/acp-8-2895-2008>
- Zhang Y, Liu P, Pun B, Seignur C (2006) A comprehensive performance evaluation of MM5-CMAQ for the summer 1999 southern oxidants study episode—part I: evaluation protocols, databases, and meteorological predictions. *Atmos Environ* 40:4825–4838. <https://doi.org/10.1016/j.atmosenv.2005.12.043>
- Zhang H, Chen G, Hu J, Chen SH, Wiedinmyer C, Kleeman M, Ying Q (2014) Evaluation of a seven-year air quality simulation using the Weather Research and Forecasting (WRF)/Community Multiscale Air Quality (CMAQ) models in the eastern United States. *Sci Total Environ* 473–474:275–285. <https://doi.org/10.1016/j.scitotenv.2013.11.121>
- Zhong M, Saikawa E, Liu Y, Naik V, Horowitz LW, Takigawa M, Zhao Y, Lin NH, Stone EA (2016) Air quality modeling with WRF-Chem v3.5 in East Asia: sensitivity to emissions and evaluation of simulated air quality. *Geosci Model Dev* 9:1201–1218. <https://doi.org/10.5194/gmd-9-1201-2016>